

Validation of charge welds and skin contamination FEM predictions in the extrusion of a AA6082 aluminum alloy

Marco Negrozio^{1,a*}, Riccardo Pelaccia^{2,b}, Lorenzo Donati^{1,c}, Barbara Reggiani^{2,d}, Sara Di Donato^{1,e}

¹ DIN Department of Industrial Engineering - University of Bologna, Viale Risorgimento 2, 40136, Bologna, Italy

² DISMI Department of Sciences and Methods for Engineering - University of Modena and Reggio Emilia, Via Amendola 2, 42122, Reggio Emilia, Italy

^amarco.negozio2@unibo.it, ^briccardo.pelaccia@unimore.it, ^cl.donati@unibo.it, ^dbarbara.reggiani@unimore.it, ^esara.didonato2@unibo.it

Keywords: Extrusion, Aluminum Alloy, FEM Simulation, Charge Welds, Skin Contamination

Abstract. The reduction of scraps related to Charge Welds and Skin Contamination defects is getting an increased industrial attention in order to improve the extrusion process overall efficiency. Recently, FEM simulations allowed the prediction of these defects under different die designs or processing conditions without performing time-consuming and expensive experimental analysis. However, the validation of the FEM codes has not been fully experimentally assessed. In this paper, Charge Welds and Skin Contamination defects were experimentally analysed in the extrusion of a AA6082 aluminum alloy profile produced under strictly monitored processing conditions. The collected data were used to assess the accuracy of the predictions made by using two commercial FEM codes Qform Extrusion UK and Altair HyperXtrude. The final aim of this work is to discuss the reliability of the FEM simulations and to validate their applicability in the industrial field.

Introduction

The extrusion of lightweight alloys represents a widely used forming process to produce profiles with constant cross-section, high geometry complexity and excellent mechanical properties. During an extrusion cycle, at the beginning and the end of each extruded profile, defects may occur affecting the properties of the components and leading to the scrap of material [1, 2].

“Charge Welds” (fig. 1) are an intrinsic defect caused by the continuous extrusion of consecutive billets [3]. At the end of each ram stroke, after the removal of the billet rest, the die remains completely filled with the already extruded material. When the next billet is loaded into the container and the extrusion starts, the new material interacts with the old one present in the die thus generating a transition zone where the profile contains a mixture of new and old billet material. This transition zone is defined as Charge Welds extent. The part of the extruded profile in which this interaction is present must be discarded because it is usually contaminated by oxides, dust, or lubricant collected during the loading into the press, thus resulting in the lowering of the mechanical properties. The scrap of material due to the Charge Welds defect usually starts from the stop mark, which is a visible surface defect generated during the billet change due to the contact between the material and the die bearings, and ends when the cross-section of the profiles contains only the new billet material (Fig. 1c).



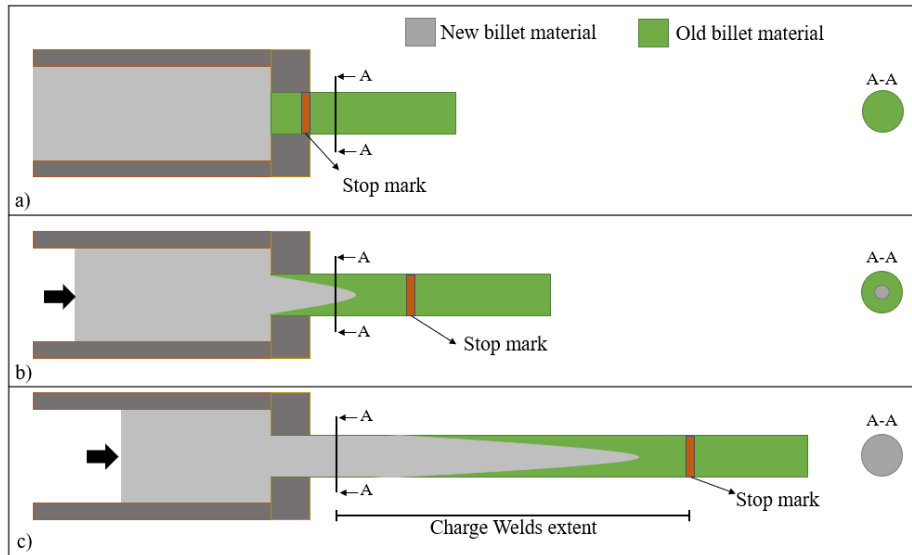


Figure 1: Schematization of the Charge Welds generation. a) Start of the extrusion process, b) interaction between new and old billet material in the profile, c) Charge Welds extent.

The second type of defect investigated in this work is known as “Billet Skin Contamination” as depicted in fig. 2. It is related to the outer layer (i.e. ‘skin’) of the billets which has a different chemical composition and microstructure with respect to the inner billet material due to the DC-casting process conditions and, if not specifically removed, it may also contain contaminations as oxides, dust or impurities collected in the billet pre-heating and handling phases [4]. During the ram stroke, if the billet rest is too short, the billet skin can flow inside the die until it reaches the extruded profile, thus generating a decrease of the mechanical proprieties and, consequently, the scrap of material on the right side of the stop mark. Indeed, by analysing the Fig. 2a, it is possible to notice that the skin contamination may occur before the stop mark at the end of the ram stroke thus increasing the length of the profile to be discarded. If the billet rest is too long, there is no contamination on the profile but uncontaminated billet material is discarded in the billet rest (Fig. 2c). Fig. 2b represents the optimized condition with no billet sin contamination in the profile before the stop mark and also a minimal thickness of the billet rest.

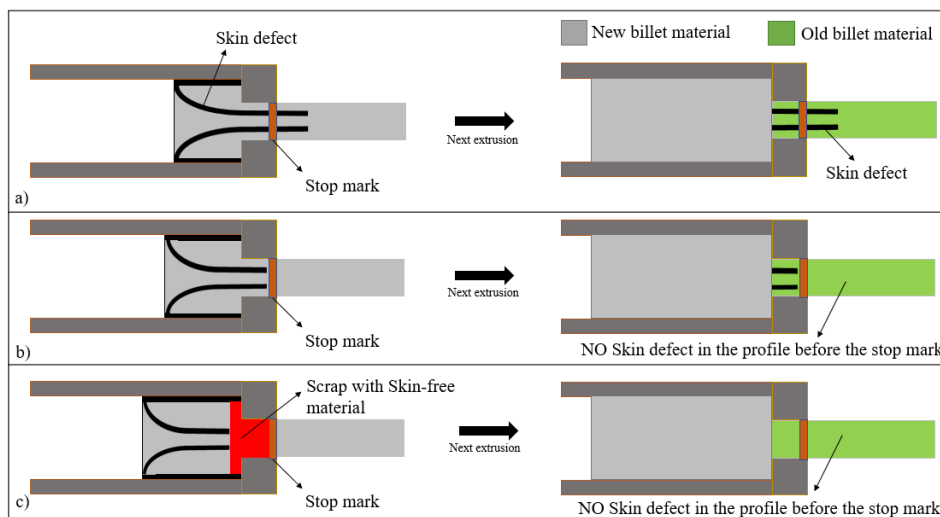


Figure 2: Schematization of the Skin Contamination generation. a,c) Unoptimized billet rest, b) optimized billet rest.

Table 1: Process parameters and geometry tolerances.

Process Parameters and geometry tolerances	Profile
Aluminum alloy	AA6082
Extrusion ratio	20
Ram speed [mm/s]	7.64
Container temperature [°C]	440
Billet initial temperature [°C]	530
Die initial temperature [°C]	450
Ram acceleration time [s]	5
Billet length [mm]	990
Billet diameter [mm]	254
Container diameter [mm]	264
Billet Rest length [mm]	15

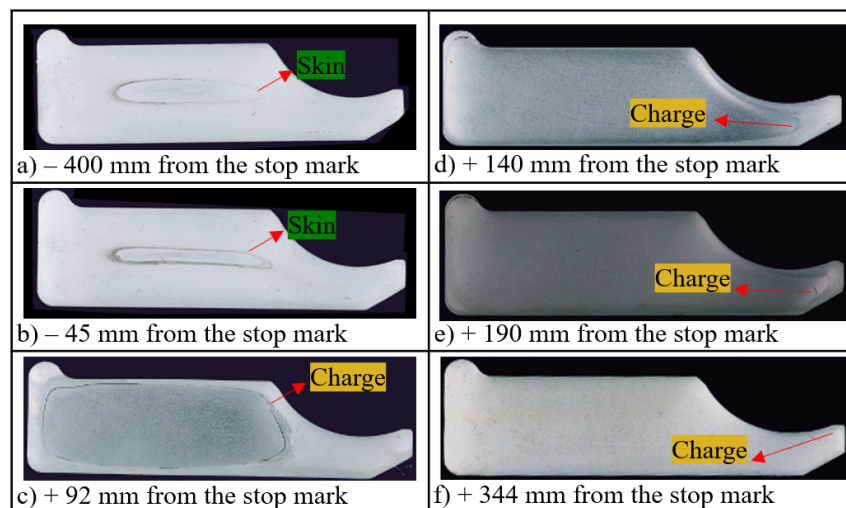


Figure 4: Cross-section of the profiles after etching: evolution of Skin Contamination and Charge Welds defects.

Fig. 5 reports the behaviours of the defects within the profile section at different distances from the stop mark: negative values on the x-axis represent samples extracted from the end of the billet 6th (billet skin defect) while positive ones represent samples extracted from the transition from billet 6th to 7th (charge weld defect). In the y-axis the percentage of profile section contaminated area by the defects is reported while the vertical lines represent the extremes of the scrap made by the company based on the experience of the technicians. The figure shows a clear unoptimized amount of profile length scrap since both the Charge Welds and the Skin Contamination extents are lower than the scrap made by the company. The Charge defect appears in the center of the cross-section of the profile and starts at +70 mm from the stop mark, increasing rapidly until it reaches the 90% of contamination at +190 mm and up to 95% at +400 mm, which is considered the defect extinction. The Skin Contamination also appears in the center of the profile at -3700 mm from the stop mark. The main difference between the two defects is that the Skin remained nearly constant in terms of contaminated area (12-15%) until it flattened out towards the shorter sides (4.5% at +68 mm), thus suggesting the upcoming of the Charge Welds defect.

To evaluate the Skin Contamination behaviour during the extrusion, a slice of the billet taken from the experimental batch was also analysed: a specimen of the billet surface was extracted, polished, and etched to assess the initial billet skin thickness. A value of 250 µm was found as skin depth in the billet.

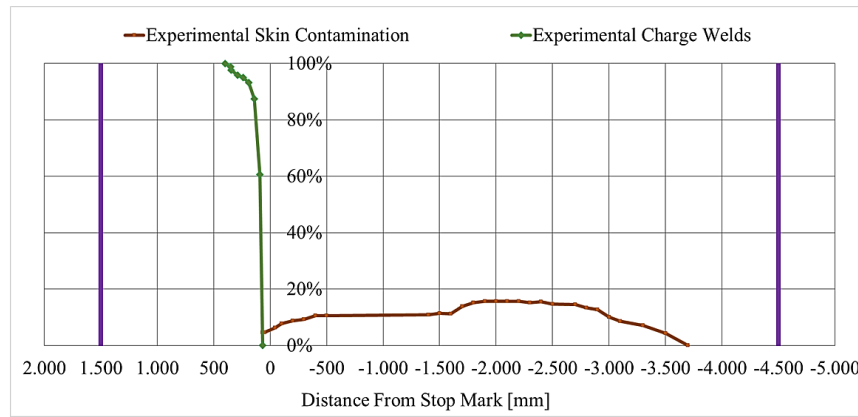


Figure 5: Experimental evolutions of the Charge Welds and Skin Contamination compared to the industrial scrap (purple lines in the graph).

Numerical and Analytical Investigation

The investigated case study was simulated using two commercial FEM codes: Qform Extrusion UK (Fig. 6a) and Altair HyperXtrude (Fig. 6b). The first FEM code is a Qform tool tailored for the simulation of the extrusion process. Through the use of this tool, it is possible to automatically generate the mesh and perform thermomechanical simulations using an ALE (Arbitrarian-Lagrangian-Eulerian) approach. The same numerical approach is used by HyperXtrude, which is an Altair product also focused on the extrusion simulation. Both codes are capable of simulating the material flow, the thermal field, the extrusion load and several extrusion defects, including Charge Welds and Skin Contamination starting from the CAD geometries of workpiece-tools and the definition of the process parameters.

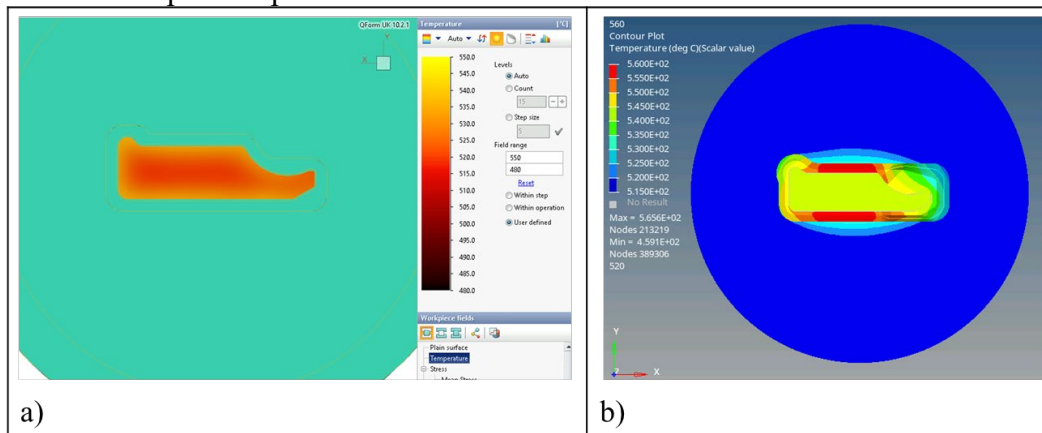


Figure 6: Temperature simulation using: a) Qform Extrusion UK, b) Altair HyperXtrude.

Both simulations were made using the same flow stress law: the following Hensel-Spittel equation was selected because it considers the effect of strain, strain rate and temperature [9]:

$$\bar{\sigma} = A \cdot e^{m_1 T} \cdot \bar{\epsilon}^{-m_2} \cdot \dot{\bar{\epsilon}}^{-m_3} \cdot e^{\frac{m_4}{\bar{\epsilon}}} \cdot (1 + \bar{\epsilon})^{m_5 T} \cdot e^{m_7 \bar{\epsilon}} \cdot \dot{\bar{\epsilon}}^{m_8 T} \cdot T^{m_9} \quad (1)$$

where $\bar{\sigma}$ is the flow stress, $\bar{\epsilon}$ the strain, $\dot{\bar{\epsilon}}$ the strain rate, T the temperature (K) and A, m_1 - m_9 the material parameters to be regressed over experimental trials. These material parameters were taken from [10] and are summarized in Tab. 2.

Table 2: AA6082 Hensel-Spittel parameters [12].

Hensel-Spittel Parameters	AA6082
A	568000 [MPa]
m1	-0.002117 [K ⁻¹]
m2	0.1059
m3	0.098
m4	0.0009266 [K ⁻¹]
m5	-0.00065
m7	0.02343
m8	0.00006471[K ⁻¹]
m9	-1.208

Table 3: Friction conditions [10].

Surface	Friction condition
Billet-Container	Sticking condition
Billet-Ram	Sticking condition
Billet-Die	Sticking condition
Bearings	Levanov model (m = 0.3, n = 1.25)

The friction conditions between workpiece and tools were taken from [10]. The optimized default values for extrusion are reported in Tab. 3 while the AA6082 physical properties used in the simulations are reported in Tab. 4.

Table 4: Material parameters for the AA6082 aluminum alloy [10].

Material Properties	AA6082
Density [Kg/m ³]	2690
Specific heat [J/kg K]	900
Thermal conductivity [W/m K]	200
Thermal expansivity [m/K]	2.34*10 ⁻⁵
Young's modulus [GPa]	68.9
Poisson's ratio	0.33

Results and Discussion

At first, the results of the simulations were validated by comparing the experimental and numerical exit temperature. The experimental data were acquired during multiple billets extrusion, although only the transition between the 6th and 7th was etched and analysed. Table 5 reports the average profile exit temperature including its standard deviation during the steady-state phase of three consecutive billets extruded in the same process conditions. The temperatures were acquired by the use of a pyrometer pointed in the top part of the profile immediately after the press exit. Table 5 also reports the average peak extrusion load for the same three investigated billets (5th, 6th and 7th). The simulation results show an error in the prediction of the two parameters always below the 5% using both FEM codes.

Table 5: Comparison of profile exit temperature and maximum extrusion load.

	Altair HyperXtrude	Qform Extrusion UK	Experimental
Profile Exit Temperature [°C]	542 (1.2% error)	529 (1.1% error)	535 ±5
Max Extrusion Load [MN]	17.5 (2.3% error)	17.7 (3.5% error)	17.1 ±0.1

After validating the simulations, the numerical predictions of the Charge Welds and Skin Contamination made by using Qform Extrusion UK and Altair HyperXtrude were carried out and the results are reported in Fig. 6 and Fig. 7. Both data are compared to the experimentally found values of the defects' evolutions.

According to the Qform Extrusion UK simulation, the Charge Welds onset was found at +85 mm and its extinction at +280 mm, showing a slight overestimation of 15 mm for onset and an underestimation of 120 mm for the defect extent. The Skin Contamination extent was predicted at -3500 mm while it was experimentally found at -3700 mm, with an underestimation of 200 mm.

Moreover, the numerical predictions show that the percentage evolution is accurate both in the case of Charge Welds and Skin Contamination (Fig. 7).

According to the Altair HyperXtrude simulation, the Charge Welds onset was found at +92 mm and its extinction at +406 mm, showing an overestimation of 22 mm for onset and of 6 mm for the defect extent. The Skin Contamination extent was predicted at -4500 mm while it was experimentally found at -3700 mm, with an overestimation of 800 mm. The numerical prediction of the Charge Welds shows a great accuracy in the percentage evolution simulation, while the Skin Contamination results were less accurate since the defect does not enlarge till the 100% of the sample area but remains almost constant at around the 14% (Fig. 8). This significant difference was caused by the increase in the Skin volume calculated by the code during the ram stroke, while it is supposed to remain constant during the entire process.

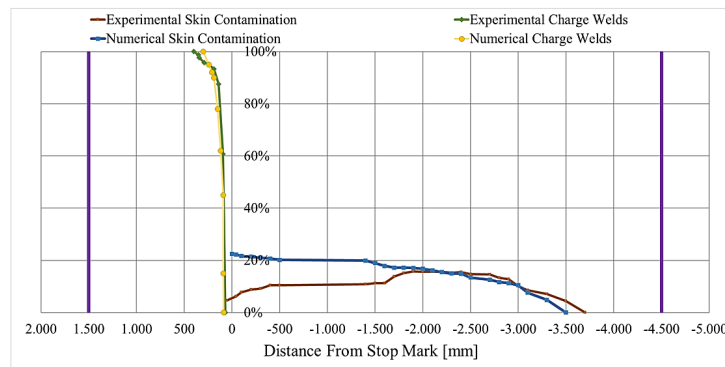


Figure 7: Qform Extrusion UK

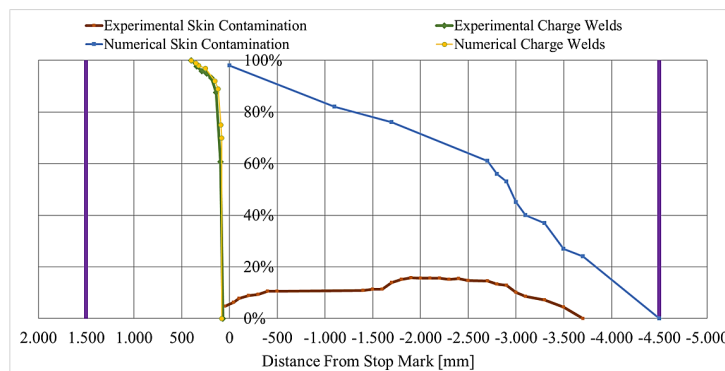


Figure 8: Altair HyperXtrude

The numerical simulations show an accuracy considerably higher if compared to the scrap made by technician's experience. The industrial error on the Charge Welds extent is 1100 mm while the Qform and HyperXtrude predictions errors are 120 mm and 6 mm, respectively. Moreover, the industrial error on the Skin Contamination extent is 800 mm while the Qform and HyperXtrude predictions errors are 200 mm and 800 mm, respectively. In summary, the error in the simulation is always lower than the one made by the industrial scrap except in the prediction made by Altair HyperXtrude on the Skin Contamination prediction, which resulted the same as the industrial one.

Conclusions

In the present work, experimental and numerical investigations were carried out for evaluating the accuracy of the Qform Extrusion UK and Altair HyperXtrude FEM codes in the prediction of Charge Welds and Skin Contamination evolutions on a solid extruded profile made by AA6082 aluminum alloys. The main outcomes of this work can be summarized as follows:

- A very good correlation between experimental and numerical data on Charge Welds predictions, both in terms of extent and of percentage evolution, was confirmed using the two tested FEM codes. 120 mm of error was found in the defect extent prediction using Qform Extrusion UK while 6 mm using Altair HyperXtrude. Both discrepancies with the experimental defect extent were extremely lower than the one found considering the industrial scrap (1100 mm).
- A good numerical-experimental matching was found for the Skin Contamination defect: Qform Extrusion UK accurately predicted both the extent of the defect (with an error of 200 mm) and its percentage evolution. However, Altair HyperXtrude prediction was less accurate in the defect extent (with error of 800 mm, the same as the industrial scrap) and in its percentage evolution.
- The numerical investigations proved the reliability of the FEM codes for the extrusion process optimization thus proving their applicability in the industrial field. Further experimental and numerical analyses are still required to assess the accuracy of the FEM simulation in different 6XXX aluminum alloys extrusions.

References

- [1] N. Hashimoto, Application of Aluminum Extrusions to Automotive Parts, Kobelco Technology Review 35 (2017) 69-75.
- [2] J. Hirsch, Automotive trends in aluminium - The European perspective, Materials Forum 28(3) (2004) 15-23.
- [3] A.J. Den Bakker, L. Katgerman, S. Van Der Zwaag, Analysis of the structure and resulting mechanical properties of aluminium extrusions containing a charge weld interface, Journal of Material Processing Technology 229 (2016) 9-21.
<https://doi.org/10.1016/j.jmatprotec.2015.09.013>
- [4] Y.T. Kim, K. Ikeda, Flow behavior of billet surface layer in porthole die extrusion of aluminum. Metall Mater Trans A 31(6) (2000) 1635-1643. <https://doi.org/10.1007/s11661-000-0173-4>
- [5] B. Reggiani, L. Donati, Experimental, numerical, and analytical investigations on the charge weld evolution in extruded profiles. International Journal of Advanced Manufacturing Technology 99 (2018) 1379-1387. <https://doi.org/10.1007/s00170-018-2595-4>
- [6] A.A. Ershov, V.V. Kotov, YuN. Loginov. Capabilities of QForm-extrusion based on an example of the extrusion of complex shapes, Metallurgist, 2012, 55(9-10), p 695-701.
<https://doi.org/10.1007/s11015-012-9489-8>
- [7] P. Chaturanga. Case study of extrusion die design optimization using innovative cartridge type die, Light Metal Age, 2014, 77(5), p 20-27.
- [8] N. Biba, S. Stebunov, A. Lishny, Simulation of material flow coupled with die analysis in complex shape extrusion, Key Engineering Materials, 2014, 585, p 85-92.
<https://doi.org/10.4028/www.scientific.net/KEM.585.85>
- [9] A. Hensel, T. Spittel, Kraft und Arbeitsbedarf bildsamer Formgebungsverfahren, 1. Auflage, Leipzig: VEB Deutscher Verlag für Grundstoffindustrie, 1978.
- [10] M. Negozio, R. Pelaccia, L. Donati, B. Reggiani, T. Pinter, L. Tomesani, Finite Element Model Prediction of Charge Weld Behaviour in AA6082 and AA6063 Extruded Profiles, Journal of Material Engineering and Performance 30 (2021) 4691-4699. <https://doi.org/10.1007/s11665-021-05752-x>